Electrochemical Studies of Nickel(II) and Cobalt(II) Complexes of Tetra-azamacrocycles bearing a Pyridine Functional Group and *X*-Ray Structures of $[Ni^{II}(L^3)Cl]ClO_4$ and $[Ni^{II}(L^3)][ClO_4]_2{\cdot}H_2O$ {L^3 = *meso*-2,3,7,11,12-Pentamethyl-3,7,11,17-tetra-azabicyclo[11.3.1]heptadeca-1(17),13,15-triene}†

Chi-Ming Che,* Shing-Tat Mak, Wai-On Lee, and Kwok-Wing Fung
Department of Chemistry, University of Hong Kong, Pokfulam Road, Hong Kong
Thomas C. W. Mak*
Department of Chemistry, The Chinese University of Hong Kong, Shatin, New Territories, Hong Kong

The new complexes $[Ni^{II}(L^3)Cl]ClO_4$ (**1**), $[Co^{II}(L^3)(CH_3CN)][ClO_4]_2$, and $[Ni^{II}(L^3)][ClO_4]_2{\cdot}H_2O$ (**2**) {L^3 = *meso*-2,3,7,11,12-pentamethyl-3,7,11,17-tetra-azabicyclo[11.3.1]heptadeca-1(17),13,15-triene} have been prepared. Their redox chemistry and electrocatalytic behaviour in the CO_2 reduction process were studied in comparison with related cobalt(II)– and nickel(II)–tetra-azamacrocyclic systems. The complex cation in (**1**) [monoclinic, space group $P2_1/n$, a = 9.457(4), b = 17.614(3), c = 14.078(4) Å, β = 107.39(2)°, Z = 4, R = 0.065 for 2 812 observed Mo-K_α data] is isostructural with the distorted tetragonal pyramidal Co^{II} analogue. The increased atomic number of the nickel centre is reflected in a significant shortening (by *ca.* 0.03 Å) of the metal–N bond distances. In (**2**) [monoclinic, space group $P2_1/c$, a = 10.248(1), b = 17.958(4), c = 13.538(3) Å, β = 90.48(2)°, Z = 4, R = 0.076 for 3 310 observed Mo-K_α data] the two independent ClO_4^- groups are bridged by the water molecule through hydrogen bonding, and one ClO_4^- group is unidentately bound to the 'square-planar' metal atom by a long Ni–O bond of 2.838(7) Å. The macrocyclic L^3 ligand adopts different conformations in (**1**) and (**2**): the substituted methyl groups at N(2) and N(4) are oriented *anti* with respect to each other in (**1**), but bear a *syn* relationship in (**2**).

Macrocyclic systems derived from 2,6-diacetylpyridine such as L^1, 2,12-dimethyl-3,7,11,17-tetra-azabicyclo[11.3.1]heptadeca-1(17),2,11,13,15-pentaene, L^2, *meso*-2,12-dimethyl-3,7,11,17-tetra-azabicyclo[11.3.1]heptadeca-1(17),13,15-triene, and L^3, *meso*-2,3,7,11,12-pentamethyl-3,7,11,17-tetra-azabicyclo-[11.3.1]heptadeca-1(17),13,15-triene (Figure 1) have been subjected to extensive investigation[1–3] in the past. Few studies, however, have been carried out employing this class of ligand in transition-metal complexes in homogeneous catalysis. We have recently been interested in the chemistry of low-valent transition-metal complexes containing saturated tetra-azamacrocycles. The pyridine functional group in L^3 may be expected to help in stabilizing the electron-rich metal centre through π-back bonding. The synthesis of L^3 and *X*-ray structural and electrochemical studies on $[Co^{II}(L^3)Cl]ClO_4$ have previously been described.[3] In this paper we report the redox chemistry and structural features of the cobalt(II)–L^3 and nickel(II)–L^3 complexes. Their electrocatalytic behaviour in the CO_2 reduction process is also compared with that of the unsaturated Co^{II}–L^1 and Ni^{II}–L^1 systems.

Experimental

The ligand L^3 and complexes $[Co^{II}(L^1)(CH_3CN)][ClO_4]_2$, $[Ni^{II}(L^1)][ClO_4]_2$, $[Co^{III}(L^2)Cl_2]ClO_4$, and $[Co^{III}(L^1)X_2]ClO_4$ (X = Cl, Br, or NCS) were prepared as previously described.[1–3] All reagents used were of analytical grade, and elemental analyses of the newly prepared complexes were performed by the Australian National Laboratory.

Preparations.—$[Co^{II}(L^3)(CH_3CN)][ClO_4]_2$. $Co(ClO_4)_2{\cdot}xH_2O$ (0.3 g) and L^3 (0.3 g) were heated in water (25 cm^3) at *ca.* 70 °C for 20 min. Upon addition of $NaClO_4$ (5 g) and cooling to 0 °C, dark purple crystals appeared. These were filtered off and recrystallised by slow diffusion of diethyl ether into an acetonitrile solution of the crude product (yield *ca.* 50%) (Found: C, 40.4; H, 5.7; Cl, 11.4; N, 12.0. Calc. for $C_{20}H_{35}Cl_2CoN_5O_8$: C, 39.8; H, 5.8; Cl, 11.8; N, 11.6%). U.v.–visible spectral data in CH_3CN, $\lambda_{max.}$/nm($\varepsilon_{max.}$/dm^3 mol^{-1} cm^{-1}): 575 (100), 483 (250), 337 (1 730), 237 (11 200). I.r. (Nujol mull): ν(C≡N), 2 240; ν(C=C) and ν(C=N), 1 610 and 1 580 cm^{-1}.

$[Ni^{II}(L^3)Cl]ClO_4$ (**1**) *and* $[Ni^{II}(L^3)][ClO_4]_2{\cdot}H_2O$ (**2**). $NiCl_2{\cdot}xH_2O$ (0.3 g) and L^3 (0.3 g) were heated in MeOH (25 cm^3) at *ca.* 50 °C for 15 min. Upon addition of $LiClO_4$, a green precipitate of $[Ni(L^3)Cl]ClO_4$ appeared. This was filtered off

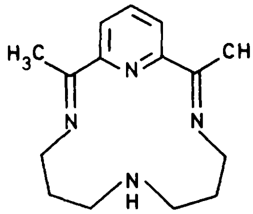

L^1

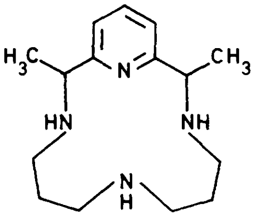

L^2

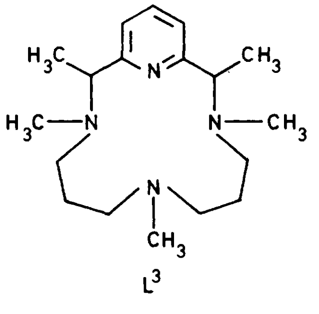

L^3

---

† *Supplementary data available:* see Instructions for Authors, *J. Chem. Soc., Dalton Trans.*, 1988, Issue 1, pp. xvii—xx.

Table 1. Data collection and processing parameters*

Formula	$[Ni(C_{18}H_{32}N_4)Cl]ClO_4$ (**1**)	$[Ni(C_{18}H_{32}N_4)][ClO_4]_2 \cdot H_2O$ (**2**)
M	498.09	580.09
a/Å	9.457(4)	10.248(1)
b/Å	17.614(3)	17.958(4)
c/Å	14.078(4)	13.538(3)
β/°	107.39(2)	90.48(2)
U/Å^3	2 238(1)	2 491.4(8)
Z	4	4
D_m (flotation)/g cm^{-3}	1.48	1.53
D_c/g cm^{-3}	1.478	1.546
Space group	$P2_1/n$	$P2_1/c$
μ/cm^{-1}	11.41	10.49
Crystal size (mm)	0.32 × 0.28 × 0.18	0.41 × 0.32 × 0.21
Mean μr	0.14	0.17
Transmission factors	0.710—0.749	0.595—0.653
No. of unique data measured	3 289	3 820
No. of data observed with $\|F\| > 3\sigma(\|F\|)$, n	2 812	3 310
No. of variables, p	277	322
F(000)	1 047.8	1 215.8
$R = \Sigma\|\|F_o\| - \|F_c\|\|/\Sigma\|F_o\|$	0.065	0.076
Weighting scheme, w	$[\sigma^2(\|F_o\|) + 0.0010\|F_o\|^2]^{-1}$	$[\sigma^2(\|F_o\|) + 0.0015\|F_o\|^2]^{-1}$
$R' = [\Sigma w(\|F_o\| - \|F_c\|)^2/w\|F_o\|^2]^{\frac{1}{2}}$	0.083	0.105
$S = [\Sigma w(\|F_o\| - \|F_c\|)^2/(n - p)]^{\frac{1}{2}}$	1.866	2.094
Residual peaks in final difference map/e Å^{-3}	+1.58 to −0.55	+1.71 to −0.50

* Features common to both: scan type, ω–2θ; scan speed, 2.02—8.37° min^{-1}; scan range, 1° below $K_{\alpha 1}$ to 1° above $K_{\alpha 2}$; background, stationary counts for half the scan time at each end; collection range, h, k, $\pm l$; $2\theta_{max.} = 50°$.

Table 2. Atomic co-ordinates (× 10^5 for Ni; × 10^4 for other atoms) for $[Ni(L^3)Cl]ClO_4$ (**1**)

Atom	x	y	z
$[Ni(L^3)Cl]^+$ ion			
Ni	36 412(8)	21 697(4)	−2 811(5)
Cl(1)	6 018(2)	1 862(1)	675(1)
N(1)	1 735(5)	2 712(3)	−527(4)
N(2)	2 537(5)	1 429(3)	463(4)
N(3)	3 480(5)	1 497(3)	−1 513(3)
N(4)	4 181(5)	3 222(3)	−869(4)
C(1)	1 640(7)	3 419(3)	−848(6)
C(2)	421(8)	3 871(4)	−842(7)
C(3)	−658(9)	3 565(4)	−526(7)
C(4)	−559(9)	2 800(5)	−208(7)
C(5)	649(7)	2 389(4)	−231(5)
C(6)	891(7)	1 550(4)	−22(6)
C(7)	2 938(8)	621(3)	389(5)
C(8)	2 785(8)	347(3)	−645(5)
C(9)	3 831(8)	700(4)	−1 146(5)
C(10)	4 699(8)	1 716(5)	−1 924(5)
C(11)	4 635(9)	2 514(5)	−2 335(5)
C(12)	5 182(12)	3 066(7)	−1 506(9)
C(13)	2 912(11)	3 580(6)	−1 374(13)
C(14)	2 948(11)	4 499(6)	−1 439(10)
C(15)	−143(10)	1 192(5)	449(8)
C(16)	2 971(9)	1 656(4)	1 511(5)
C(17)	2 047(8)	1 519(4)	−2 313(5)
C(18)	5 185(14)	3 632(5)	−108(10)
Perchlorate ion			
Cl(2)	2 158(2)	−562(1)	2 904(2)
O(1)	2 095(11)	−1 307(4)	3 148(7)
O(2)	3 538(8)	−330(4)	2 867(7)
O(3)	1 146(11)	−395(7)	2 041(8)
O(4)	1 842(13)	−145(5)	3 651(9)

and the orange filtrate was reduced in volume to 10 cm^3. Upon cooling to 0 °C, orange crystals of $[Ni^{II}(L^3)][ClO_4]_2 \cdot H_2O$, together with a small amount of green solid, gradually deposited. Both complexes were recrystallised by slow diffusion of diethyl ether into an acetonitrile solution of the crude product (total yield *ca.* 70%). For $[Ni^{II}(L^3)Cl]ClO_4$ (green) (Found: C, 43.2; H, 6.5; Cl, 14.5; N, 11.2. Calc. for $C_{18}H_{32}Cl_2N_4NiO_4$: C, 43.4; H, 6.4; Cl, 14.3; N, 11.3%). U.v.–visible spectral data in CH_3CN, $\lambda_{max.}$/nm ($\varepsilon_{max.}$/dm^3 mol^{-1} cm^{-1}): 399 (160), 262 (5 880), 224 (5 570). I.r. (Nujol mull): ν(C=C) and ν(C=N), 1 617 and 1 590 cm^{-1}. For $[Ni^{II}(L^3)][ClO_4]_2 \cdot H_2O$ (orange) (Found: C, 38.3; H, 5.7; Cl, 12.5; N, 10.0. Calc. for $C_{18}H_{34}Cl_2N_4NiO_9$: C, 38.5; H, 5.7; Cl, 12.6, N, 10.0%). U.v.–visible spectral data in CH_3CN, $\lambda_{max.}$/nm($\varepsilon_{max.}$/dm^3 mol^{-1} cm^{-1}): 480 (200), 231 (10 710). I.r. (Nujol mull): ν(C=C) and ν(C=N), 1 610 and 1 580 cm^{-1}.

Physical Measurements.—Cyclic voltammetric measurements were performed using a PAR universal programmer (model 175), potentiostat (model 173), and digital coulometer (model 179). Formal potentials were taken from the mean values of the cathodic and anodic peak potentials at 25 °C at a scan rate of 100 mV s^{-1}; the measurements were made against a Ag–$AgNO_3$ (0.1 mol dm^{-3} in acetonitrile) electrode with ferrocene as the internal standard. Acetonitrile (Mallinkrodt Chrom A.R.) for electrochemical studies was distilled over CaH_2. The supporting electrolyte was either $[NBu_4]BF_4$ (0.1 mol dm^{-3}) or $[NBu_4]ClO_4$ (0.1 mol dm^{-3}).

For the detection of carbon monoxide, a Shimadzu GC-8A gas chromatograph equipped with a f.i.d. (flame ionization detector) was used. The conditions for the g.c. (gas chromatographic) analysis are: column, 4 ft of 5 Å molecular sieve (80—100 mesh); N_2 gas flow rate, 30 cm^3 min^{-1}; oven temperature, 70 °C. A Hamilton 1-cm^3 gas-tight syringe was used for sample injection. Owing to the low sensitivity of the f.i.d., the CO, after separation from the gas mixture, was reduced to CH_4 with H_2 in the presence of a nickel catalyst, which was contained in a 4 × 1/8 in stainless steel tube at a temperature of 370 °C inside an insulated steel box.[4]

X-*Ray Structural Studies.*—The two nickel complexes, $[Ni^{II}(L^3)Cl]ClO_4$ (**1**) and $[Ni^{II}(L^3)][ClO_4]_2 \cdot H_2O$ (**2**), were handled in the same manner. Diffraction measurements were made on a Nicolet R3m four-circle diffractometer (graphite-monochromatised Mo-K_α radiation, $\lambda = 0.710\ 69$ Å), and determination of the crystal class, orientation matrix, and accurate unit-cell parameters were performed according to established procedures.[5]

Intensities were recorded at 22 °C, and data collection and processing parameters are summarised in Table 1. The raw intensities were processed with the learnt-profile procedure,[6] and absorption corrections based on a pseudo-ellipsoidal fit to azimuthal scans of selected strong reflections over a range of 2θ values.[7]

Structure refinement of (**1**) proceeded with the parameters of the isomorphous Co^{II} complex.[2] The structure of (**2**) was solved by Patterson and Fourier methods. For each complex, all non-hydrogen atoms in the asymmetric unit were subjected to anisotropic refinement. The hydrogen atoms of the macrocyclic ligand were generated geometrically (C–H fixed at 0.96 Å) and included in structure-factor calculations with assigned isotropic thermal parameters; the methyl groups were treated as rigid groups, and the remaining hydrogen atoms were allowed to ride on their respective parent carbon atoms. The water protons of (**2**) did not show up in the final difference map.

All computations were performed on a Data General Nova 3/12 minicomputer with the SHELXTL systems.[8] Analytic expressions of neutral-atom scattering factors incorporating the real and imaginary components of anomalous dispersion were employed.[9] Blocked-cascade least-squares refinement[10] converged to the *R* indices and other parameters listed in Table 1.

Table 3. Atomic co-ordinates (× 10^5 for Ni; × 10^4 for other atoms) for $[Ni(L^3)][ClO_4]_2 \cdot H_2O$ (**2**)

Atom	*x*	*y*	*z*
$[Ni(L^3)]^{2+}$ ion			
Ni	21 683(7)	15 517(4)	18 960(5)
N(1)	2 498(4)	2 530(3)	1 546(3)
N(2)	3 998(5)	1 604(3)	2 384(4)
N(3)	1 796(6)	513(3)	2 273(4)
N(4)	406(5)	1 791(3)	1 380(4)
C(1)	1 468(7)	2 978(4)	1 353(4)
C(2)	1 678(10)	3 690(4)	1 030(6)
C(3)	2 984(10)	3 936(4)	931(5)
C(4)	3 993(8)	3 477(4)	1 170(5)
C(5)	3 727(6)	2 759(3)	1 476(4)
C(6)	4 696(6)	2 178(4)	1 733(5)
C(7)	4 760(7)	900(4)	2 354(6)
C(8)	4 188(10)	275(5)	2 828(7)
C(9)	2 924(14)	17(5)	2 168(12)
C(10)	812(12)	211(6)	1 552(9)
C(11)	−592(9)	533(6)	1 643(8)
C(12)	−704(7)	1 355(5)	1 812(7)
C(13)	224(6)	2 627(4)	1 578(5)
C(14)	−117(8)	2 782(5)	2 669(6)
C(15)	5 945(7)	2 470(6)	2 191(6)
C(16)	3 900(7)	1 892(5)	3 420(5)
C(17)	1 229(12)	493(6)	3 269(8)
C(18)	409(8)	1 729(5)	262(5)
Perchlorate ions			
Cl(1)	7 674(2)	3 840(1)	−261(1)
O(1)	6 505(8)	4 229(5)	−191(10)
O(2)	8 661(11)	4 323(8)	−370(13)
O(3)	7 817(11)	3 731(7)	784(7)
O(4)	7 577(16)	3 167(6)	−585(12)
Cl(2)	3 505(2)	931(1)	−871(1)
O(5)	3 341(8)	1 192(6)	65(5)
O(6)	2 516(7)	1 207(5)	−1 489(5)
O(7)	4 739(7)	1 105(6)	−1 250(7)
O(8)	3 422(10)	162(5)	−822(10)
Water molecule			
O(w1)	7 032(11)	1 547(8)	−103(12)

The final atomic co-ordinates for compounds (**1**) and (**2**) are listed in Tables 2 and 3 respectively. Selected bond distances, bond angles, and torsion angles for the two complexes are compared in Table 4. Additional material available from the Cambridge Crystallographic Data Centre comprises H-atom co-ordinates, thermal parameters, and remaining bond lengths and angles.

Results and Discussion

The Co^{II} and Ni^{II} complexes of L^3 were readily prepared by reaction of the divalent metal salts with L^3 in CH_3CN or CH_3OH. The reaction between $Ni(ClO_4)_2$ and L^3 in CH_3OH–H_2O (10:1) at *ca.* 50 °C gave a pale violet-red solution ($\lambda_{max.}$,

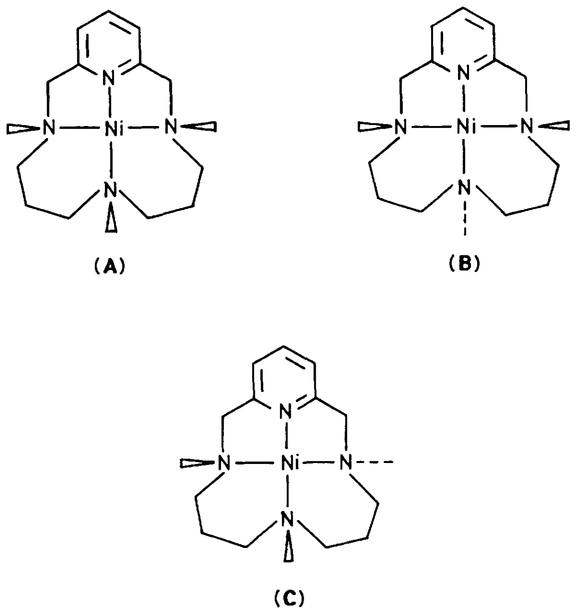

Figure 1. Structures of the Ni^{II} complexes of 3,7,11-trimethyl-3,7,11,17-tetra-azabicyclo[11.3.1]heptadeca-1(17),13,15-triene

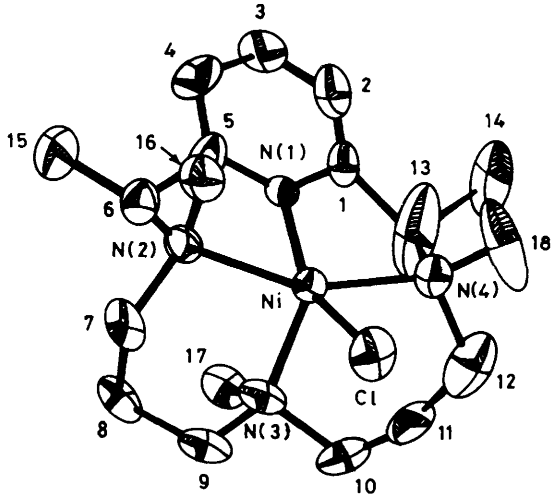

Figure 2. Molecular structure and atom numbering of the $[Ni^{II}(L^3)Cl]^+$ cation in (**1**)

Table 4. Selected bond lengths (Å), bond angles (°), and torsion angles (°) in (**1**) and (**2**)

(*i*) Complex cations*

	(**1**)	(**2**)		(**1**)	(**2**)
Ni–L	2.312(2)	2.838(7)	N(3)–C(17)	1.481(7)	1.473(12)
Ni–N(1)	1.977(5)	1.852(5)	Ni–N(3)	2.068(5)	1.972(5)
Ni–N(2)	2.132(5)	1.985(5)	Ni–N(4)	2.153(5)	1.978(5)
N(1)–C(1)	1.319(8)	1.350(8)	N(1)–C(5)	1.344(9)	1.329(7)
C(1)–C(2)	1.403(10)	1.369(10)	C(4)–C(5)	1.360(11)	1.383(9)
C(2)–C(3)	1.342(13)	1.417(14)	C(3)–C(4)	1.415(11)	1.360(12)
C(1)–C(13)	1.615(18)	1.457(9)	C(5)–C(6)	1.512(9)	1.479(9)
N(4)–C(13)	1.354(11)	1.537(9)	N(2)–C(6)	1.516(8)	1.537(8)
N(4)–C(12)	1.512(15)	1.504(10)	N(2)–C(7)	1.484(8)	1.487(9)
C(11)–C(12)	1.487(14)	1.498(14)	C(7)–C(8)	1.499(10)	1.423(12)
C(10)–C(11)	1.515(12)	1.557(15)	C(8)–C(9)	1.509(11)	1.635(17)
N(3)–C(10)	1.486(10)	1.499(13)	N(3)–C(9)	1.499(8)	1.468(14)
C(13)–C(14)	1.622(15)	1.546(11)	C(6)–C(15)	1.476(14)	1.511(10)
N(4)–C(18)	1.401(12)	1.517(9)	N(2)–C(16)	1.464(9)	1.499(8)
L–Ni–N(1)	153.1(2)	85.0(3)	L–Ni–N(3)	99.7(1)	95.5(3)
N(3)–Ni–N(2)	97.9(2)	98.2(2)	N(3)–Ni–N(4)	97.9(2)	96.8(2)
L–Ni–N(2)	96.0(1)	84.0(3)	L–Ni–N(4)	97.2(1)	97.6(3)
N(1)–Ni–N(2)	80.0(2)	82.3(2)	N(1)–Ni–N(4)	79.2(2)	82.6(2)
N(1)–Ni–N(3)	107.2(2)	179.3(2)	N(2)–Ni–N(4)	157.4(2)	164.6(2)
C(1)–N(1)–C(5)	121.7(6)	122.8(5)	C(2)–C(3)–C(4)	120.2(8)	120.3(7)
N(1)–C(1)–C(2)	120.4(7)	119.5(7)	N(1)–C(5)–C(4)	120.5(6)	119.9(6)
C(1)–C(2)–C(3)	118.8(7)	118.2(8)	C(3)–C(4)–C(5)	118.4(8)	119.0(7)
N(1)–C(1)–C(13)	109.8(7)	112.8(6)	N(1)–C(5)–C(6)	112.9(6)	113.6(5)
C(2)–C(1)–C(13)	129.0(7)	127.6(7)	C(4)–C(5)–C(6)	126.5(7)	126.4(6)
C(1)–C(13)–N(4)	110.0(11)	106.1(5)	C(5)–C(6)–N(2)	107.5(5)	107.0(5)
C(13)–N(4)–C(12)	112.8(9)	110.3(5)	C(6)–N(2)–C(7)	110.6(5)	107.9(5)
N(4)–C(12)–C(11)	116.8(8)	113.2(7)	N(2)–C(7)–C(8)	115.1(5)	116.1(7)
C(12)–C(11)–C(10)	110.0(7)	116.8(8)	C(7)–C(8)–C(9)	115.8(5)	107.7(8)
C(11)–C(10)–N(3)	116.2(6)	115.5(9)	C(8)–C(9)–N(3)	116.0(6)	113.4(9)
C(10)–N(3)–C(9)	105.1(5)	104.1(8)	N(1)–Ni–N(3)	107.2(2)	179.3(2)
Ni–L–Cl(2)		161.2(7)			
N(1)–C(1)–C(13)–N(4)	−38.2(11)	−32.0(7)	N(1)–C(5)–C(6)–N(2)	37.8(8)	−22.2(7)
C(1)–C(13)–N(4)–C(12)	156.1(8)	166.6(5)	C(5)–C(6)–N(2)–C(7)	−161.2(6)	159.9(5)
C(13)–N(4)–C(12)–C(11)	−66.4(11)	179.8(7)	C(6)–N(2)–C(7)–C(8)	67.1(8)	−173.4(7)
N(4)–C(12)–C(11)–C(10)	−72.5(10)	29.0(12)	N(2)–C(7)–C(8)–C(9)	66.2(8)	70.0(9)
C(12)–C(11)–C(10)–N(3)	79.2(9)	42.0(13)	C(7)–C(8)–C(9)–N(3)	−75.0(7)	−74.8(12)
C(11)–C(10)–N(3)–C(9)	−178.9(5)	168.6(9)	C(8)–C(9)–N(3)–C(10)	177.4(5)	175.5(9)
C(11)–C(10)–N(3)–C(17)	62.7(7)	48.0(11)	C(8)–C(9)–N(3)–C(17)	−64.5(7)	−66.9(11)
N(1)–C(1)–C(13)–C(14)	−164.6(7)	88.6(7)	N(1)–C(5)–C(6)–C(15)	171.2(6)	−148.6(6)
C(1)–C(13)–N(4)–C(18)	−90.8(10)	−74.2(6)	C(5)–C(6)–N(2)–C(16)	77.2(7)	−79.0(6)
C(14)–C(13)–N(4)–C(18)	27.1(18)	167.0(6)	C(15)–C(6)–N(2)–C(16)	−54.7(8)	48.3(7)

(*ii*) Hydrogen bonding

	(**1**)	(**2**)		(**1**)	(**2**)
O(w1) · · · O(4)		3.03(2)	O(4) · · · O(w1) · · · O(7)		107(2)
O(w1) · · · O(7)		2.92(2)	O(w1) · · · O(4)–Cl(1)		147(1)
			O(w1) · · · O(7)–Cl(2)		126(1)

* For (**1**), L = Cl(1); for (**2**), L = O(5), see Figures 2 and 3.

345 and 500 nm). However, an attempt to isolate a pure product from this solution was not successful. The presence of co-ordinated CH_3CN in $[Co(L^3)(CH_3CN)][ClO_4]_2$ was confirmed by its i.r. band at 2 240 cm^{-1}.[11]

Barefield and co-workers[3a] and Moore and co-workers[3b] recently reported their structural studies on Ni^{II} complexes of a related macrocyclic amine, 3,7,11-trimethyl-3,7,11,17-tetra-azabicyclo[11.3.1]heptadeca-1(17),13,15-triene. Three different forms, (**A**), (**B**), and (**C**), with structures shown in Figure 1, were obtained. Figure 2 shows an ORTEP plot of the complex cation in $[Ni^{II}(L^3)Cl]ClO_4$ (**1**) with the atomic numbering scheme. In comparison with its cobalt(II) analogue,[2] the $[Ni^{II}(L^3)Cl]^+$ cation has the same metal–chloride bond length, the increased atomic number of the nickel(II) atom being reflected in a significant shortening of the remaining metal–ligand distances involving the quadridentate macrocycle, by *ca.* 0.03 Å. The structures of (**1**) and (**B**) are similar, with the same orientation of the N–CH_3 groups. The measured Ni–Cl bond distance in (**1**), 2.312(2) Å, is in the usual range found in most five-co-ordinate Ni^{II} complexes; for example, *d*(Ni–Cl) lies between 2.350 and 2.314 Å in $[Ni(C_7H_{15}N_2)(H_2O)Cl_3]$.[12]

Figure 3 shows an ORTEP plot of the complex cation in $[Ni(L^3)][ClO_4]_2 \cdot H_2O$ (**2**). The two independent perchlorate groups are bridged by the water molecule through hydrogen bonding (Table 4), and one of the perchlorates is unidentately bound to the metal atom through O(5). The molecular packing of (**2**) is illustrated in Figure 4. The co-ordination geometry about the Ni atom in (**2**) is square pyramidal, with O(5) at the apex and the metal centre virtually co-planar with the N atoms of the macrocyclic ligand (Figure 3). The long Ni–O(5) bond

Table 5. Formal reduction potentials of the cobalt and nickel complexes in 0.1 mol dm^{-3} $[NBu_4]BF_4$ in acetonitrile

	Potentials/V *vs.* $[Fe(\eta\text{-}C_5H_5)_2]^+$–$[Fe(\eta\text{-}C_5H_5)_2]$		
	Metal-centred couple		
Complex	M^{III}–M^{II}	M^{II}–M^{I}	Ligand-centred couple[a]
$[Ni^{II}(L^1)][ClO_4]_2$		−1.62	−1.02
$[Ni^{II}(L^3)Cl]ClO_4$	0.97[b]	−1.34	
$[Ni^{II}(L^3)][ClO_4]_2$	1.29	−1.28	
$[Co^{II}(L^3)(CH_3CN)][ClO_4]_2$	1.14[b]	−1.64	
$[Co^{III}(L^2)Cl_2]ClO_4$	−0.56	−1.97	
$[Co^{III}(L^1)Cl_2]ClO_4$	−0.51	−1.91	−0.92
$[Co^{III}(L^1)Br_2]ClO_4$	−0.41	−1.91	−0.96
$[Co^{III}(L^1)(NCS)_2]ClO_4$	−0.40	−1.92	−0.94
$[Co^{II}(L^1)(CH_3CN)][ClO_4]_2$		−1.90	−0.94

[a] The reduction of the L^1 ligand. [b] Irreversible.

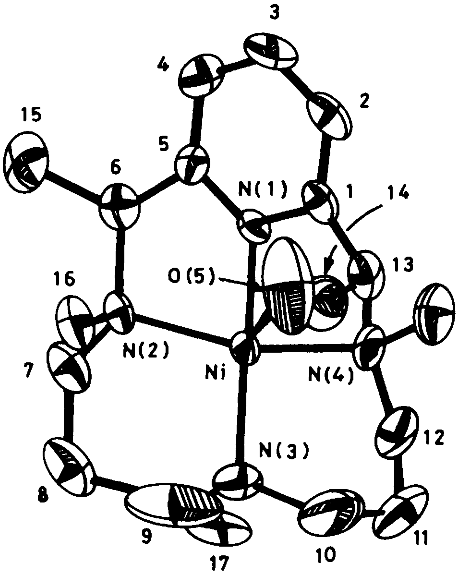

Figure 3. Molecular structure and atom numbering of the $[Ni^{II}(L^3)]^{2+}$ cation in (**2**). The bonding of the metal atom with an oxygen atom of a perchlorate group is also illustrated

distance and large Ni–O(5)–Cl(2) angle indicate a relatively weak metal–perchlorate interaction[13,14] as a result of the weak donor strength of the perchlorate ion. The Ni–N distances in (**2**) are about 0.13 Å shorter than the corresponding distances in (**1**).

The macrocyclic ligand in (**2**) adopts a conformation which differs from the C_s configuration in (**1**) (Figure 3) in that the substituted methyl groups at N(2) and N(4) are oriented *anti* with respect to each other (Figure 3). When the two complexes are compared, it is seen that the angle Cl–Ni–N(1) in (**1**) [153.1(2)°] is much greater than O(5)–Ni–N(1) in (**2**) [85.0(3)°]. This increase in ligand–metal–N(pyridyl) bond angle from (**2**) to (**1**) may lead to an inversion of the bonding configuration of N(2), so that the methyl groups at N(2) and N(4) now bear a *syn* relationship. A more precise description of the conformational change undergone by the macrocyclic ligand, which corresponds to the change in co-ordination geometry from square pyramidal in (**2**) to tetragonal pyramidal in (**1**), is provided by the torsion angles given in Table 4.

Interestingly, the disposition of the N–CH_3 groups in (**2**) is the same as that in the structure of (**C**), recently structurally characterised by Moore and co-workers.[3b] These two complexes have the same orange colour and similar optical spectra in solution [$\lambda_{max.}$/nm(ε/dm^3 mol^{-1} cm^{-1}): (**2**), 480 (200); (**C**),[3] 475 (233)].

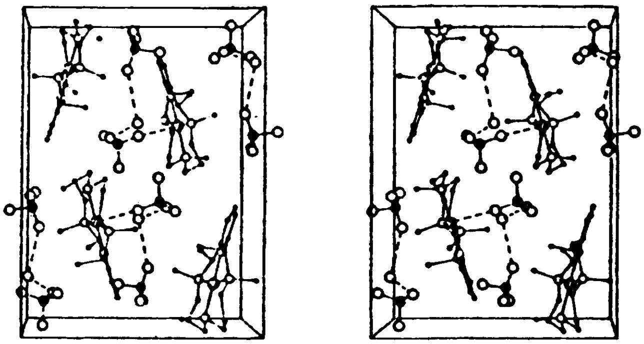

Figure 4. Stereoview of the molecular packing in $[Ni^{II}(L^3)][ClO_4]_2\cdot H_2O$ (**2**). The origin of the unit cell lies at the upper left corner, with *a* pointing towards the reader, *b* downwards, and *c* from left to right. The metal–perchlorate and water–perchlorate bonding interactions are represented by broken lines

Electrochemistry.—Table 5 summarises the formal reduction potentials of the newly prepared and related metal complexes. The cyclic voltammograms of $[Co^{II}(L^3)(CH_3CN)]^{2+}$ and $[Ni(L^3)]^{2+}$ in acetonitrile [Figure 5(*a*) and (*b*)] show a reversible–quasi-reversible reduction couple (ΔE_p *ca.* 60—70 mV, $i_{p,a}/i_{p,c} \approx 1$, scan rate = 50—200 mV s^{-1}) at −1.64 V and −1.28 V *vs.* $[Fe(\eta\text{-}C_5H_5)_2]^+$–$[Fe(\eta\text{-}C_5H_5)_2]$ respectively. Because L^3 is σ-saturated and electroinactive in this potential range, the electrode reactions are metal centred and attributed to the reduction of M^{II} to M^I (M = Co and Ni). The electrochemistry of cobalt and nickel complexes of L^1 has previously been discussed; the reduction of the unsaturated L^1 macrocycle has been found at −0.95 to −1.1 V.[1,15]

An interesting finding that emerges from the present electrochemical work is that the $E_{\frac{1}{2}}$ values of the cobalt(II) and nickel(II) complexes of L^3 are substantially higher (*ca.* 300 mV) than their corresponding L^1 analogues despite the fact that the unsaturated L^1 ligand is a better electron acceptor than the σ-saturated L^3 tertiary amine. The unusually high redox potentials of transition-metal tertiary amine complexes has previously been rationalised on the basis of 'solvation effects'.[16] Thus the L^3 tertiary amine is a good ligand system for the stabilisation of low-valent transition-metal ions.

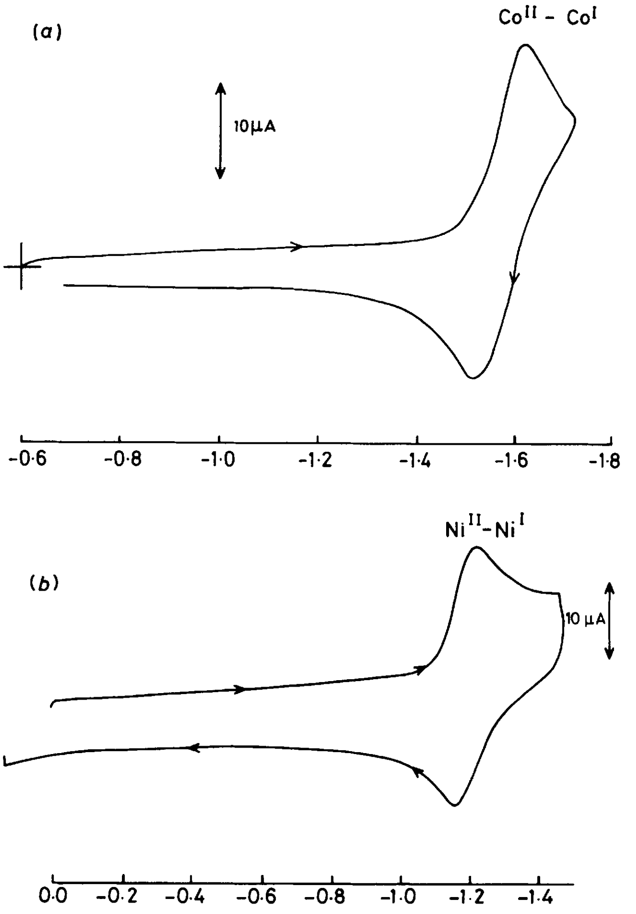

Figure 5. Cyclic voltammograms of (*a*) $[Co^{II}(L^3)(CH_3CN)]^{2+}$ and (*b*) $[Ni^{II}(L^3)]^{2+}$ (1 mmol) in 0.1 mol dm^{-3} $[NBu_4]BF_4$ in acetonitrile solution. Working electrode, pyrolytic graphite; scan rate, 100 mV s^{-1}

Recent work has shown that cobalt(II) and nickel(II) tetra-azamacrocyclic complexes are good catalysts for the electro-reduction of CO_2 to CO.[17-19] Figure 6(*a*) and (*b*) show the cyclic voltammograms of $[Co^{III}(L^1)Cl_2]ClO_4$ in the presence and absence of CO_2. In Figure 6(*a*), there are three reversible–quasi-reversible reduction couples (I), (II), and (III), with potentials at −0.51, −0.92, and −1.91 V respectively. With reference to previous work,[1,14] couple (III) is attributed to the reduction of Co^{II} to Co^{I}. In the presence of CO_2, the Co^{II}–Co^{I} couple becomes irreversible and a large catalytic reductive wave at −1.90 V is found. This catalytic reductive wave is due to the reduction of CO_2 by the electrogenerated Co^{I} species, since CO (identified by g.c.) was obtained with 20—30% current efficiency by controlled-potential electrolysis of an acetonitrile solution of $[Co^{III}(L^1)Cl_2]ClO_4$ (40 cm^3, 1 mmol) saturated with CO_2 at −1.90 V for 0.5 h. Hydrogen was not detected as a by-product. Other Co–L^2 and Ni–L^1 complexes were also found to be active for the electroreduction of CO_2.[20] However, the cyclic voltammograms of acetonitrile solutions of $[Ni(L^3)]^{2+}$ and $[Co^{II}(L^3)(CH_3CN)]^{2+}$ are not affected by CO_2 even with a scan rate of 10 mV s^{-1}, indicating that the electrogenerated Ni^{I} and Co^{I} species are relatively inactive towards CO_2. This lack of reactivity may be argued by the presence of N–CH_3 groups on L^3, that sterically hinder the binding of CO_2 to the metal centre. Thus the macrocyclic tertiary amine, on one hand stabilises low-valent metal ion by slowing down the demetallation reaction, yet on the other exerts a strong steric effect between the N–CH_3 groups and the substrate (CO_2 in this case). This is important when one considers the future use of this class of compounds in homogeneous catalysis.

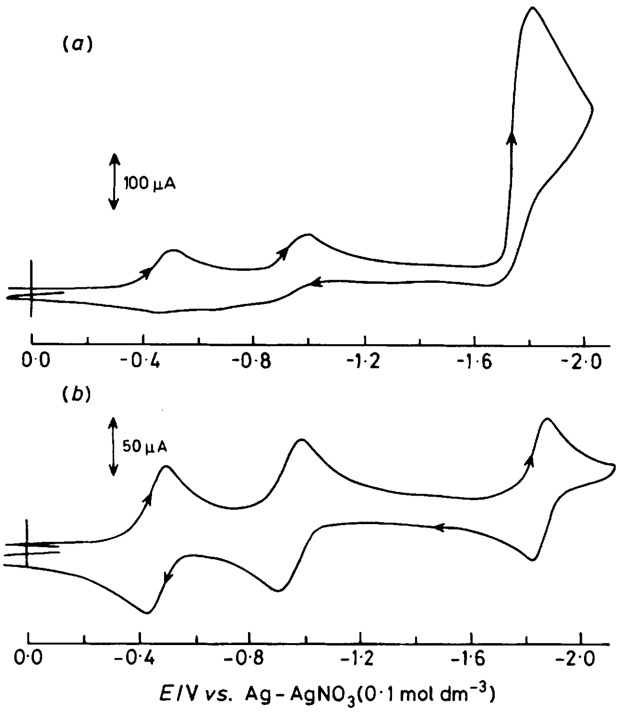

Figure 6. Cyclic voltammogram of $[Co^{III}(L^1)Cl_2]ClO_4$ (*ca.* 1 mmol) in 0.1 mol dm^{-3} $[NBu_4]BF_4$ in acetonitrile solution in (*a*) the presence and (*b*) the absence of CO_2. Working electrode, pyrolytic graphite; scan rate, 100 mV s^{-1}

Acknowledgements

Financial support (C-M. C., S-T. M., and W-O. L.) by the Committee of Conference and Research Grants of the University of Hong Kong is acknowledged. W-O. L. acknowledges the receipt of a scholarship, ministered by the Croucher Foundation.

References

1 K. M. Long and D. H. Busch, *Inorg. Chem.*, 1970, **9**, 505; J. L. Karn and D. H. Busch, *ibid.*, 1969, **8**, 1149; E. K. Barefield, F. V. Lovecchio, N. E. Tokel, E. Ochiai, and D. H. Busch, *ibid.*, 1972, **11**, 283; J. L. Karn and D. H. Busch, *Nature (London)*, 1966, **211**, 160.
2 C. M. Che, S. T. Mak, and T. C. W. Mak, *Inorg. Chem.*, 1986, **25**, 4705.
3 (*a*) K. A. Foster, E. K. Barefield, and D. G. V. Derveer, *J. Chem. Soc., Chem. Comm.*, 1986, 680; (*b*) N. W. Alcock, P. Moore, and H. A. Omar, *J. Chem. Soc., Dalton Trans.*, 1987, 1107.
4 K. Porter and D. H. Volman, *Anal. Chem.*, 1962, **34**, 749.
5 R. A. Sparks, in 'Crystallographic Computing Techniques,' ed. F. R. Ahmed, Munksgaard, Copenhagen, 1976, p. 452.
6 R. Diamond, *Acta Crystallogr., Sect. A*, 1969, **25**, 43.
7 G. Kopfmann and R. Huber, *Acta Crystallogr., Sect. A*, 1968, **24**, 348; A. C. T. North, D. C. Phillips, and F. S. Mathews, *ibid.*, p. 351.
8 G. M. Sheldrick, in 'Computational Crystallography,' ed. D. Sayre, Oxford University Press, New York, 1982, p. 506.
9 'International Tables for *X*-Ray Crystallography,' Kynoch Press, Birmingham, 1973, vol. 4, pp. 55 and 149.
10 J. W. Schilling, in 'Crystallographic Computing,' ed. F. R. Ahmed, Munksgaard, Copenhagen, 1970, p. 201.
11 See, for example, C. M. Che, K. Y. Wong, and T. C. W. Mak, *J. Chem. Soc., Chem. Commun.*, 1985, 546; R. E. Clark and P. C. Ford, *Inorg. Chem.*, 1970, **9**, 227.

12 F. K. Ross and G. D. Stucky, *Inorg. Chem.*, 1969, **8**, 2734.
13 D. A. Wright and J. D. Quinn, *Acta Crystallogr., Sect. B*, 1974, **30**, 2132.
14 D. L. Lewis and D. J. Hodgson, *Inorg. Chem.*, 1974, **13**, 143.
15 F. V. Lovecchio, E. S. Gore, and D. H. Busch, *J. Am. Chem. Soc.*, 1974, **96**, 3109.
16 N. Jubran, G. Ginzburg, H. Cohen, and D. Meyerstein, *J. Chem. Soc., Chem. Commun.*, 1982, 517; E. K. Barefield, G. M. Freeman, and D. G. V. Derveer, *Inorg. Chem.*, 1986, **25**, 552.
17 M. Beley, J-P. Collin, R. Ruppert, and J-P. Sauvage, *J. Chem. Soc., Chem. Commun.*, 1984, 1315.
18 B. Fisher and R. Eisenberg, *J. Am. Chem. Soc.*, 1980, **102**, 7361.
19 M. Beley, J-P. Collin, R. Ruppert, and J-P. Sauvage, *J. Am. Chem. Soc.*, 1986, **108**, 7461.
20 C. M. Che and W. O. Lee, unpublished work.

Received 7th August 1987; *Paper* 7/1467